

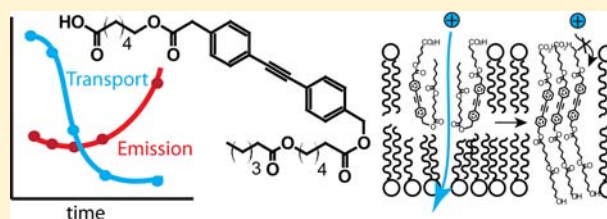
# Mechanism of Ion Transport by Fluorescent Oligoester Channels

Joanne M. Moszynski and Thomas M. Fyles\*

Department of Chemistry, University of Victoria, Victoria, British Columbia V8P 5C2, Canada

**S** Supporting Information

**ABSTRACT:** The synthesis and membrane activity of a suite of linear oligoesters containing a common diphenylacetylene unit core and differing in the hydroxyl terminus are reported. Active compounds formed high-conductance channels efficiently in both vesicle and planar bilayers, with one compound showing a very unusual slow loss of transport activity over a 20–30 min period. Steady-state and time-resolved fluorescence studies establish the rapid partition of active compounds to the bilayer and identify at least three types of membrane-associated species by their differing fluorescence lifetimes. The change in the distribution of species is correlated with the slow loss of activity. The results are interpreted in terms of an aggregate within a single bilayer leaflet that is nonetheless competent to transport ionic species through the bilayer. The properties of such structures, revealed by these compounds, appear to be consistent with commonly observed behaviors of other synthetic ion channels.



## INTRODUCTION

Transmembrane ion transport mediated by synthetic ion channels has been achieved by a very diverse array of structural classes ranging from overtly biomimetic peptide derivatives, via ingenious macrocyclic, helical, spherical, and tubular supra-molecular structures, to simple low-molecular-weight acyclic compounds.<sup>1–9</sup> Viewed as catalysts of translocation, synthetic ion channels rival the efficiency of natural ion channels, albeit with often poorer control of substrate selectivity and unsophisticated control of activity. Nonetheless, there are now many reports of synthetic ion channels acting as antibiotics<sup>10–14</sup> and as the central component of sensors and other analytical methodologies.<sup>15,16</sup>

Despite the wide structural diversity, the functional diversity of synthetic ion channels appears to be constrained to a relatively narrow span of conductances and durations of channel openings.<sup>9</sup> The clustering evident in this analysis suggests that many different types of relatively small molecules within a bilayer give rise to remarkably similar active ion-conducting structures. This paradox highlights the key mechanistic question: what structure(s) give rise to the observed channel conductance behaviors? In some well-studied cases—the naturally occurring peptide gramicidin<sup>17</sup> and its derivatives,<sup>18,19</sup> the octaphenyl  $\beta$ -barrels,<sup>20,21</sup> or the G-quartet-based channels<sup>22,23</sup> as examples—there is a presumed tubular structure and the structure–function relationship can be overt. In other cases—such as the hydrophile channels,<sup>24–27</sup> and the synthetic chloride membrane transporter (SCMTR) anion channels,<sup>28–31</sup> the weight of a diverse collection of experimental data leads to a general mechanistic picture of some predictive power, but as the overall molecular weight of the transporter decreases, or its conformational flexibility increases, the nature of the conducting structures becomes progressively obscure. Additionally, such small or flexible transporters can exhibit “supramolecular polymorphism” in which a distribution of

active structures is probable.<sup>32</sup> Nonetheless, the ion transport functions of flexible transporters are remarkably similar to more rigid and structurally complex examples.<sup>9</sup>

Such is the case for the oligoester channels that we have investigated recently;<sup>33–38</sup> example structures are given below (Dip = ester of 4-((4-(hydroxymethyl)phenyl)ethynyl)-phenylacetic acid, Dod = ester of 12-hydroxydodecanoic acid, G(*n*) = *n*-alkyl ester of 3-hydroxyglutaric acid, Hex = ester of 6-hydroxyhexanoic acid, Oct = ester of 8-hydroxyoctanoic acid, Trip = ester of 4-((4-(3-(hydroxypropynyl)phenyl)phenyl)ethynyl)phenylacetic acid). These compounds are readily prepared by solid-phase or optimized solution chemistries, and a survey approach has resulted in a general structure–activity optimization. In parallel, the incorporation of rigid fluorophore segments into the backbone of the transporters has provided both a probe of the environment of the transporter and a substantial increase in activity.

The range of experimental data support the inference of a “working hypothesis” mechanism (Figure 1).<sup>35</sup> Favorable partition to the bilayer membrane requires a hydrophobic transporter, but initial injection of a methanolic solution of transporter also produces a competing aqueous aggregate. Monomer dissociation from this aggregate can be rate-limiting. The aqueous monomer partitions to the bilayer and can be detected in the bilayer as both a monomeric and an oligomeric species. The kinetic evidence suggests that oligomers are responsible for transport. These oligomers are sketched as membrane-spanning, in line with a general dependence of transport on the length of the oligoesters; optimal transport occurs when the transporter length is comparable to the bilayer thickness.

Received: July 6, 2012

Published: September 4, 2012

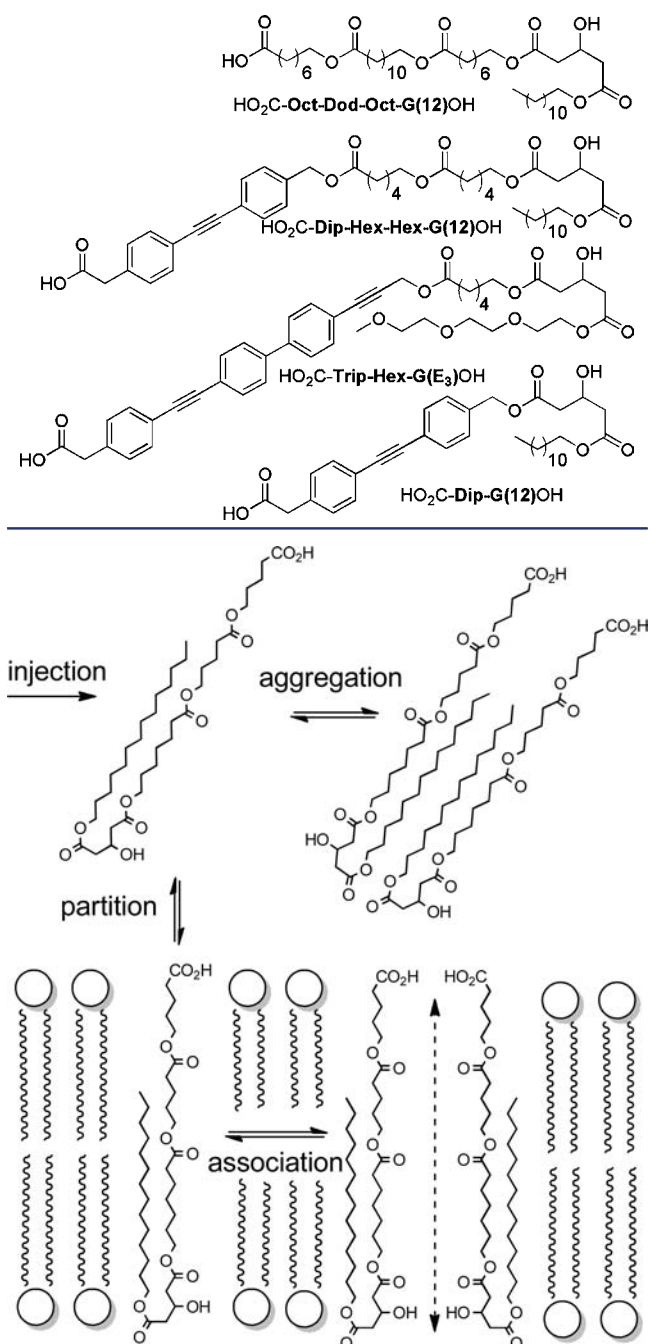


**Figure 1.** Working hypothesis for the action of oligoester channel-forming compounds on bilayer membranes.

In the absence of a more detailed structural picture, our previous investigations involved simple evolution of lead compounds through “deletion”, “mutation”, or “shuffling” of different segments. A common feature, inherited from the first active example uncovered,<sup>39</sup> has been a 3-hydroxyglutarate diester at the hydroxyl terminus of the oligoesters. Within the working hypothesis the OH group was envisaged as being capable of penetrating the bilayer to produce a membrane-spanning structure.

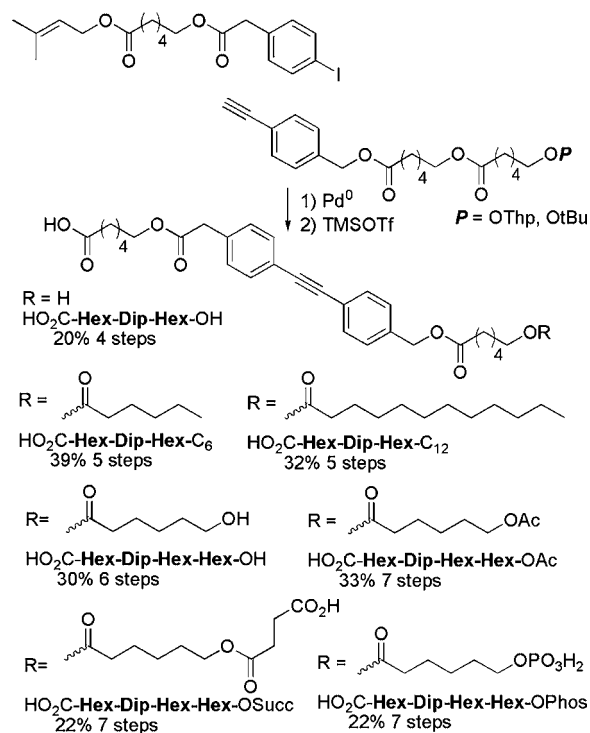
The 3-hydroxyglutarates are convenient for synthesis, but this unit and its associated mechanistic role must itself be a target for mutation. In this paper we discuss compounds in which the OH terminus is varied, and eliminated in some cases. Several active compounds have been uncovered, many of which

call into question the details of the working hypothesis. Time-resolved fluorescence studies raise further doubt on the membrane-spanning nature of the active intermediates. Our revised mechanism is consistent with all available data on oligoesters. More generally, it also responds to the question of why structurally diverse compounds exhibit very similar channel conductance characteristics.

## RESULTS AND DISCUSSION

**Synthesis.** The modular synthetic strategy involved the synthesis of several key intermediates which were elaborated into the final products using the ester coupling, deprotection, and Sonogashira reactions developed previously.<sup>35</sup> The alkyne partner (Scheme 1) was synthesized from 4-ethynylbenzyl

### Scheme 1. Structures of Prepared Compounds<sup>a</sup>



<sup>a</sup>Ac = acetyl, and tBuO = *tert*-butoxy.

alcohol and the known<sup>37</sup> tetrahydropyran-1-yl (THP)-protected 6-hydroxyhexanoic acid by ester coupling and THP deprotection. This intermediate was then diversified into two synthetic streams by utilizing standard ester or acyl chloride coupling conditions to yield a series of aromatic terminal alkynes with oligoester tails terminated by either hydroxyl or alkyl groups. Known literature procedures were then applied to functionalize the hydroxyl moiety with various substituents to form acetate-terminated, succinic acid-terminated,<sup>40</sup> or protected phosphate-terminated<sup>41</sup> triesters. The alkynes each underwent Sonogashira coupling with a previously reported<sup>33</sup> iodo compound to yield the prenyl-protected Dip-containing oligomers. After purification, trimethylsilyl (TMS) triflate<sup>42</sup> was used to remove the protecting groups to reveal the terminal carboxylic acid/phosphate and furnish the final products, the names and yields of which are shown in Scheme 1. The trivial naming of the compounds follows from the linear structures with the carboxy and hydroxy termini explicitly specified; named subunits are assumed to be linked as esters. The overall

yields of the final products range from 20% to 39% over a maximum of seven steps from the starting 4-ethynylbenzyl alcohol, and all the synthesized oligoesters were additionally purified by HPLC to give high-quality samples for further analysis. Full synthetic details are given in the Supporting Information.

**Transport in Vesicles.** The membrane activity of the new oligoesters was initially assessed by a vesicle assay to detect the compounds' ability to collapse an imposed pH gradient. Vesicle-entrapped pH-sensitive fluorescent dye HPTS (8-hydroxypyrene-1,3,6-trisulfonic acid trisodium salt) is a ratiometric sensor for internal vesicle pH in the vicinity of its  $pK_a$  (7.25). As described previously,<sup>35,36</sup> vesicles were equilibrated with added compound for a short period followed by injection of sufficient NaOH solution to impose a  $\sim 1$  pH unit gradient (basic outside). Changes in fluorescence emission were then transformed to the extent of transport from which an apparent first-order rate constant could be derived.

The activity of the compounds was assessed over a range of concentrations. As illustrated in Figure 2A, the compounds

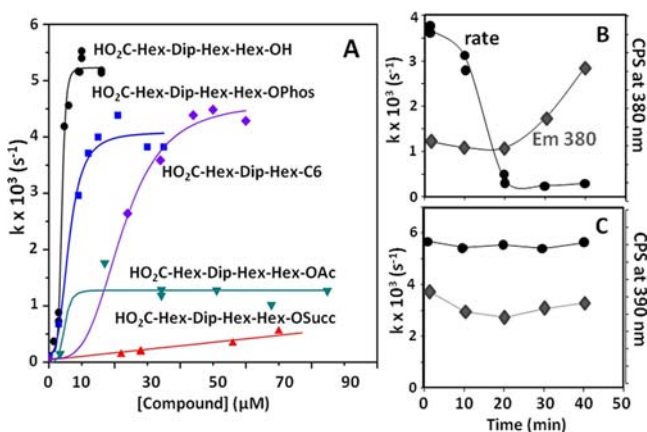


**Figure 2.** Transport activities of selected compounds assessed by the HPTS vesicle assay and time dependence of transport activity and excimer emission for two compounds: (A) HPTS-derived ion transport activity, (B) ion transport rates (black circles) compared with emission at 380 nm (gray diamonds) of 22  $\mu\text{M}$   $\text{HO}_2\text{C-Hex-Dip-Hex-C6}$ , (C) comparable data for 10  $\mu\text{M}$   $\text{HO}_2\text{C-Hex-Dip-Hex-Hex-OH}$  (gray diamonds, emission at 390 nm).

exhibited a variety of concentration-dependent behaviors. The most active examples, such as previous high-activity compounds in this class,<sup>35</sup> show a sigmoidal dependence. The sigmoidal rise in activity is indicative of a high cooperativity in channel formation, but a full analysis is precluded as the plateau region is due to aqueous aggregate formation as opposed to saturation as required for a Hill analysis.<sup>35</sup> Less active compounds show a linear concentration dependence.<sup>36</sup>

Typically a constant transport rate constant at a given concentration is expected irrespective of the delay between mixing the compound with the vesicles and the initiation of transport with the addition of base. We have previously noted that some compounds partition rather slowly and longer delays are desirable.<sup>33</sup> The compound  $\text{HO}_2\text{C-Hex-Dip-Hex-C6}$  is unusual in that it shows the opposite behavior; it has significant activity shortly after mixing, but longer delays result in a condition where the activity falls to an undetectable level. Figure 2B shows the observed rate constant as a function of the delay between mixing and the pH gradient being established.

For comparison, Figure 2C shows an invariant case for the compound  $\text{HO}_2\text{C-Hex-Dip-Hex-Hex-OH}$ . We return to this difference in behavior as other experiments are described, as it provides an important insight into the formation of the active structures.

To compare activity, we select a target rate constant ( $1 \times 10^{-3} \text{ s}^{-1}$ ) which is significantly above the detection limit and calculate from the observed concentration dependence the concentration of compound required to achieve this level of activity.<sup>35,36</sup> The results are given in Table 1.

**Table 1. Relative Activity of Compounds Assessed by the Concentration Required to Give a Target Rate Constant of  $1 \times 10^{-3} \text{ s}^{-1}$  in the HPTS Vesicle Assay<sup>a</sup>**

entry	cmpd	[cmpd] ( $\mu\text{M}$ )	rel activity
1	$\text{HO}_2\text{C-Hex-Dip-Hex-Hex-OH}$	4	2
2	$\text{HO}_2\text{C-Hex-Dip-Hex-Hex-OPhos}$	5	1.5
3	$\text{HO}_2\text{C-Hex-Dip-Hex-G(12)-OH}$	8	1
4	$\text{HO}_2\text{C-Hex-Dip-Hex-C6}$	15	0.5
5	$\text{HO}_2\text{C-Hex-Dip-Hex-Hex-OAc}$	30	0.3
6	$\text{HO}_2\text{C-Hex-Dip-Hex-Hex-OH}$	80	0.1
7	$\text{HO}_2\text{C-Hex-Dip-Hex-Hex-OSucc}$	70 (0.5) <sup>b</sup>	0.1
8	$\text{HO}_2\text{C-Hex-Dip-Hex-C12}$	n/a (50) <sup>c</sup>	n/a
9	$\text{PREO}_2\text{C-Hex-Dip-Hex-C6}$	n/a (35) <sup>c</sup>	n/a

<sup>a</sup>PRE = prenyl, 3-methylbut-2-en-1-yl. <sup>b</sup>The value in parentheses is the rate achieved ( $\times 10^3 \text{ s}^{-1}$ ) at the highest tested concentration. <sup>c</sup>The value in parentheses is the highest concentration assayed before visible precipitation occurred.

The principal result of the survey in Table 1 is that the activity of these oligoester transporters is markedly dependent on the hydroxy-terminal group. Beyond that, the functional dependence is much less clear as the same  $\text{HO}_2\text{C-Hex-Dip-Hex-Hex-X}$  core shows good activity for the neutral  $X = \text{OH}$  (entry 1), but not the neutral  $X = \text{acetyl}$  (entry 5), and good activity for  $X = \text{phosphate}$  (entry 2, dianion at this pH), but not  $X = \text{succinate}$  (entry 7, monoanion at this pH). Given the high activity of both a neutral and a dianion, the penetration of the hydroxyl terminus through the bilayer as an essential step in the transport is clearly not supported. In the shorter series (entries 4, 6, and 8), the trend likely relates to overall length and hydrophobicity, with the most hydrophobic example likely limited by the formation of an aqueous aggregate. The inactivity of the prenyl-protected compound (entry 9) might indicate that the carboxy terminus is essential, but equally might reflect the poor solubility of this compound.

**Transport in Planar Bilayers.** The three active compounds identified from the vesicle survey readily form conducting structures in planar bilayer membranes under a variety of conditions as assessed by the voltage-clamp technique. Similarly, the vesicle-inactive compound  $\text{HO}_2\text{C-Hex-Dip-Hex-C12}$  is also inactive in planar bilayers.

A few significant illustrative examples are given in Figure 3. All three active compounds show some regular "square-top" openings as shown in Figure 3A. These are generally of short duration ( $< 1 \text{ s}$ ) and small conductance relative to other behaviors ( $< 100 \text{ pS}$ ) and relatively rare (1–2% of observations); this type of opening is within the frequently observed cluster of activity derived from the literature.<sup>9</sup> Figure 3B is more typical of the behaviors as a whole. It shows two types of defined openings—one with a relatively defined range of conductances that we have previously described as "multi-

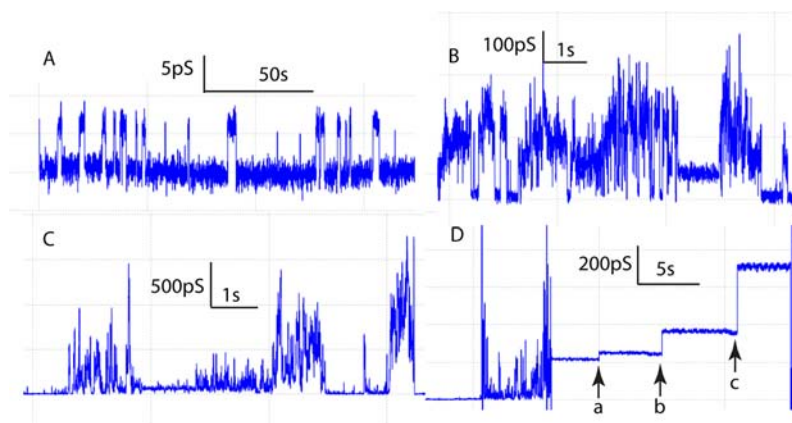


**Figure 3.** Conductance behaviors of compounds: (A) HO<sub>2</sub>C-Hex-Dip-Hex-Hex-OH, 1 M CsCl, +100 mV, 2 h after injection, (B) HO<sub>2</sub>C-Hex-Dip-Hex-Hex-OH, 1 M CsCl, +10 mV, 15 min after injection, same experiment as in (A), (C) HO<sub>2</sub>C-Hex-Dip-Hex-C6, 0.3 mol %, 1 M CsCl, +50 mV, (D) HO<sub>2</sub>C-Hex-Dip-Hex-Hex-OPhos, 0.3 mol %, 1 M CsCl, initially  $-175$  to  $-150$ ,  $-100$ , and  $-50$  mV at points a–c.

openings” and a predominant collection of “erratic” openings.<sup>9,43</sup> These events are longer ( $>1$  s), have intermediate conductance levels ( $>300$  pS), and are the dominant behavior of these compounds ( $\sim 5$ – $20\%$  multiopening;  $50$ – $75\%$  erratic). Finally, Figure 3C shows much larger conductance openings ( $>1$  nS) of the erratic type of similar durations ( $>$ seconds) which comprise about  $10\%$  of the observations.

Figure 3D shows a behavior associated only with HO<sub>2</sub>C-Hex-Dip-Hex-Hex-OPhos but present (if not recorded) in all experiments with this compound. It shows a period of steady and significant conductance lasting  $10$ – $30$  s and terminating with bilayer breakage. In the example shown, the potential was progressively changed, showing that the conductance of this type of opening is *inversely* proportional to the applied potential. This is consistent with an opening whose diameter is a balance between electrostatic repulsions between the charged head groups and the applied potential that forces masking ions into the head groups.

The overall activity of the compounds can be summarized using the activity grid methodology developed and applied previously.<sup>9,43</sup> In this approach conductance behaviors are identified according to qualitative types by assigned colors: “square-top”, green; “multiopening”, blue; “spikes”, red; “erratic”, purple (no “flicker”, yellow, events were observed). For each observed type within an experimental record, the magnitude of the conductance and the duration of the opening are determined. The results are plotted on a logarithmic activity grid spanning opening durations from  $1$  ms to  $>100$  s and conductance of  $<3$  pS to  $>3$  nS. Individual records from within a single experiment are combined over all available records and experiments to generate a summation of the activities observed. These are plotted with color density representing the frequency of a particular type of observation. Figure 4 shows the result of this analysis.

As noted above, the dominant behavior is of the erratic type, and within this group of compounds there is no significant difference in either the conductance or duration dimension. Similarly, the frequently observed spike activity is closely similar in magnitude. The differences evident in the multiopen and square-top grids are probably not significant due to the low numbers of observations. In comparison to previous summaries of activities of literature data<sup>9</sup> and of related oligoester bolaamphiphiles,<sup>43</sup> these summary grids appear to reflect the previously noted clustering about specific conductance–

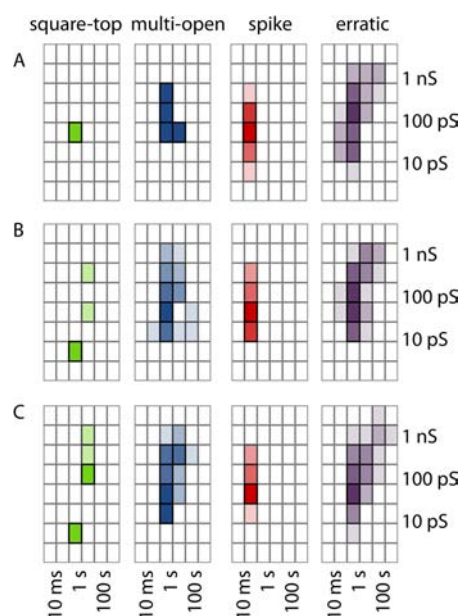


**Figure 4.** Summary activity grids of active compounds: (A) HO<sub>2</sub>C-Hex-Dip-Hex-C6, (B) HO<sub>2</sub>C-Hex-Dip-Hex-Hex-OH, (C) HO<sub>2</sub>C-Hex-Dip-Hex-Hex-OPhos.

duration values. We conclude that these compounds, capable of showing some unique characteristics at the level of a single experiment, are nonetheless within the same overall spectrum of “normal” behaviors for synthetic ion channels.

**Steady-State Fluorescence.** The inherent fluorescence of the diphenylacetylenic units in this class of oligoesters has previously been used to probe localization of the compounds as they distributed between aqueous aggregates and bilayer-associated species.<sup>35</sup> In homogeneous organic solvents, emission from a monomeric species occurs at about  $320$  nm (excitation at  $305$  nm). In aqueous solution, excimer emission from aggregates occurs at about  $380$  nm. Addition of vesicles to a solution of an aqueous aggregate of active transporters such as HO<sub>2</sub>C-Dip-Hex-Hex-G(12)OH provokes a shift from excimer emission to predominantly monomer emission, followed by a slow increase in the excimer emission. These results have been interpreted as relatively rapid monomer partition from water, followed by slow equilibration of the aqueous aggregate toward membrane-associated aggregates.<sup>35</sup>

The compounds of this paper showed the expected monomer emission in homogeneous solution, but showed a varying proportion of excimer emission in aqueous solution. The proportion of excimer followed the hydrophobicity of the hydroxyl-terminal groups: highest for HO<sub>2</sub>C-Hex-Dip-Hex-C6 and -C12, intermediate for the neutrals HO<sub>2</sub>C-Hex-Dip-Hex-OH and HO<sub>2</sub>C-Hex-Dip-Hex-Hex-OH, and virtually undetectable for the anionic HO<sub>2</sub>C-Hex-Dip-Hex-Hex-OPhos and -OSucc (see the Supporting Information). The intensity of both the monomer and the excimer emission from water is significantly lower than that from an organic solvent; thus, the partitioning of the compounds from water to vesicles results in a sharp increase in emission intensity (Figure 5A,B). The

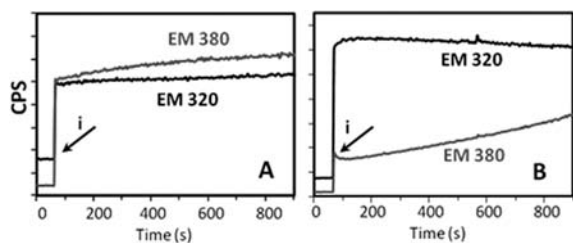


**Figure 5.** Emission spectra of compounds in the presence of vesicles. Fluorescence emission at 320 nm (black line) and 380 nm (gray line) over time of (A) 25  $\mu\text{M}$  HO<sub>2</sub>C-Hex-Dip-Hex-C12 and (B) 25  $\mu\text{M}$  HO<sub>2</sub>C-Hex-Dip-Hex-C6, injected at time *i* into an aqueous suspension of lipid vesicles (10 mM Na<sub>3</sub>PO<sub>4</sub>, 100 mM NaCl, pH 6.4).

subsequent change in the relative intensity of the monomer and excimer emissions depends on the nature of the compound. The very hydrophobic and transport-inactive compound HO<sub>2</sub>C-Hex-Dip-Hex-C12 shows little change, consistent with the previous proposal that decomposition of an aqueous aggregate is rate-limiting for very hydrophobic compounds. In contrast, the active transporter HO<sub>2</sub>C-Hex-Dip-Hex-C6 exhibits a slow increase of the excimer emission consistent with partitioning from water to the membrane followed by aggregation in the membrane. These changes are consistent with the previous proposal (Figure 1), tempered by the variable importance of the aqueous aggregate related to compound hydrophobicity and net charge.

Changes in spectra following compound addition to vesicles are typically observed. The most pronounced occur with HO<sub>2</sub>C-Hex-Dip-Hex-C6. The changes observed for HO<sub>2</sub>C-Hex-Dip-Hex-C6 (Figure 5 B and Supporting Information) are slow and on a time frame comparable to that of the loss of transport activity.

Both the monomer and the excimer emissions can be quenched by added copper salts in organic solvent and in water with Stern–Volmer quenching constants on the order of 1000 M<sup>-1</sup>. The extent to which vesicle bilayers protect the emitting species from quenching by the aqueous quencher is given in Table 2. In no case is the emitting species entirely protected, and in some cases, the quenching in the presence of vesicles is the same as without the membrane. Collectively, these data are consistent with a significant proportion of any membrane-associated species near the aqueous interface.

The fluorescence spectral changes can be used to quantify the apparent partition coefficient for transfer from water to the bilayer membrane. In this assay the amount of compound in water is held constant, a variable amount of lipid as vesicles is added, and the spectral changes are recorded. The changes

**Table 2.** Extent of Quenching (%) with 0.1 mM CuSO<sub>4</sub> in Aqueous Solution in the Absence (AQ) or Presence (VES) of Lipid Vesicles<sup>a</sup>

compd	Q at 320 nm		Q at 380 nm	
	AQ	VES	AQ	VES
HO <sub>2</sub> C-Hex-Dip-Hex-Hex-OH	30	18	34	15
HO <sub>2</sub> C-Hex-Dip-Hex-Hex-OPhos	41	28	29	12
HO <sub>2</sub> C-Hex-Dip-Hex-C6	31	19	52	10
HO <sub>2</sub> C-Hex-Dip-Hex-Hex-OAc	28	20	61	19
HO <sub>2</sub> C-Hex-Dip-Hex-OH	19	19	39	14
HO <sub>2</sub> C-Hex-Dip-Hex-Hex-OSucc	22	19	39	14
HO <sub>2</sub> C-Hex-Dip-Hex-C12	29	28	44	43

<sup>a</sup>Measured at  $\lambda_{\text{max,em}}$  determined in CH<sub>3</sub>OH (~320 nm) or aqueous solution (~380 nm).  $\lambda_{\text{max,ex}}$  varied minimally around 305 nm (301–305 nm).

eventually saturate, indicating full partition, and the evolution of the intensity at a given emission (monomer or excimer) can then be used to extract an apparent partition coefficient ( $K_p$ ) and the concentration of lipid at which the compound is half-extracted ( $\text{EC}_{50}$ ).<sup>44</sup> The titration data are illustrated for two active compounds in Figure 6. Both HO<sub>2</sub>C-Hex-Dip-Hex-C6

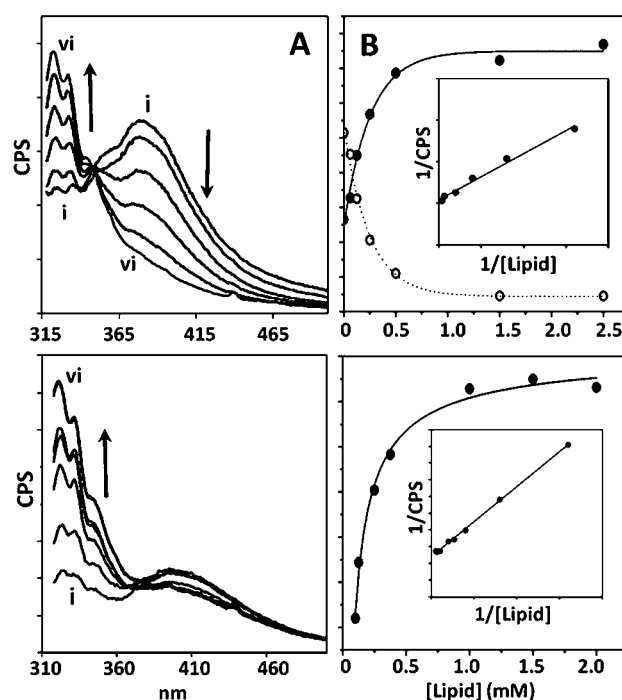


**Figure 6.** Fluorescence spectra at various lipid/compound ratios used to quantify partition equilibria. (Top) (A) Fluorescence emission spectra of 17  $\mu\text{M}$  HO<sub>2</sub>C-Hex-Dip-Hex-C6 ( $\lambda_{\text{max,ex}} = 305$  nm) titrated against lipid vesicles. From line *i* to line *vi*, [lipid] = 0.0625, 0.125, 0.25, 0.5, 1.5, and 2.5 mM. (B) Counts per second (CPS) at 320 nm (black circles) and 380 nm (open circles) as a function of [lipid], double reciprocal plot (inset) used to determine  $K_p$ . (Bottom) Analogous data for HO<sub>2</sub>C-Hex-Dip-Hex-Hex-OH.

and HO<sub>2</sub>C-Hex-Dip-Hex-Hex-OH are strongly partitioned to vesicle membranes ( $\log K_p = 6.0$  and  $5.5$ , respectively), but the difference in partition is sufficient to alter the  $\text{EC}_{50}$  values (53 and 174  $\mu\text{M}$ , respectively). At the lipid concentration of the vesicle assay (0.5 mM), the equilibrium position for both compounds is essentially fully partitioned to the membrane.

Note that the (somewhat) better partitioned compound is the less active of the pair, indicating that activity requires, but is not controlled by, the thermodynamics of the partition equilibrium.

**Fluorescence Lifetime.** The spectral changes illustrated in Figures 5 and 6 have been discussed in terms of unitary monomer and excimer emissions. Although this is approximately correct, there are clearly several processes contributing to the shape of the emission bands, particularly those lumped together as “excimer”. The magnitude of the Stern–Volmer constants observed is consistent with an emission lifetime on the order of nanoseconds, in line with literature reports.<sup>45</sup> It is known that emission lifetimes are commonly strongly influenced by the environment and that multiple lifetimes can occasionally be detected for different environments.<sup>46</sup> Typically, lifetimes are extended as the local viscosity and/or order of the environment increases. It was therefore of interest to examine the Dip fluorescence lifetime in mixtures of the compounds in vesicles to see if additional species could be inferred from the data. The technique utilized was time-correlated single photon counting (TCSPC). With accessible instrumentation, the lifetime(s) of the monomer excited state(s) lie close to the instrument response function (IRF) for homogeneous solutions in methanol. However, in the presence of vesicles, the fluorescent lifetimes of the excimer are extended and fall into an accessible time range. Initially, vesicles were prepared and equilibrated with added compound to examine the equilibrium position. Subsequently, spectra were obtained at various times following mixing of the compound with the vesicles. Some typical spectra of the latter experiments are given in Figure 7.

The data are clearly not the result of a simple exponential decay, and a fit to a sum of three exponentials gave acceptably good results for all observed data. The three processes consist of a short ( $\tau \approx 0.2\text{--}0.5$  ns), a midrange ( $\tau \approx 2.5$  ns), and a long ( $\tau \approx 3.5$  ns) component for a number of compounds and conditions. For the transport-inactive compound HO<sub>2</sub>C-Hex-Dip-Hex-C12, the relative proportions of the three components do not significantly depend on the time of incubation of the compound with the vesicles (Figure 7C). However, in the case of the transport-active HO<sub>2</sub>C-Hex-Dip-Hex-C6, the proportions do vary over the first hour following mixing (Figure 7B). In this period, the initially important “short” component falls and the “long” component increases proportionately. These spectral changes occur in the same time range as the change in transport activity and the change in proportion of excimer detected by steady-state fluorescence (Figure 2B).

**Mechanistic Possibilities.** It is clear from the vesicle transport and steady-state and time-resolved fluorescence that the working hypothesis of Figure 1 is incorrect in the number of membrane-associated species involved and therefore in the variety of processes which can influence the transport rate and efficiency. The behavior of HO<sub>2</sub>C-Hex-Dip-Hex-C6 is particularly informative of the nature of these additional species and processes. The transport activity of this compound is maximal very soon after mixing and falls off completely after 20–30 min in vesicles. In this same time period, the extent of emission from membrane-associated monomers is essentially constant and the steady-state emission from membrane-associated excimers increases and this increase is due to a shift in the proportion of species having a short-lifetime excimer emission to species having a long-lifetime excimer emission. Although correlation does not imply causation, we are tempted to associate transport activity with aggregated species which could

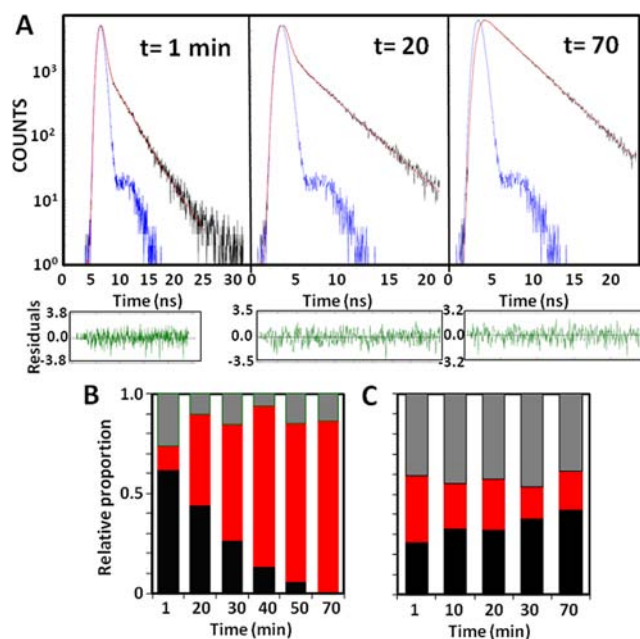


**Figure 7.** Time-resolved fluorescence lifetime measurements of compounds in vesicles: (A) TCSPC-derived fluorescence decay profiles monitored at 380 nm (276 nm excitation) for 20  $\mu\text{M}$  HO<sub>2</sub>C-Hex-Dip-Hex-C6 incubated with a suspension of lipid vesicles in aqueous buffer (10 mM Na<sub>3</sub>PO<sub>4</sub>, 100 mM NaCl, pH 6.4) (blue, IRF; black, decay; red, fit to a triexponential), (B) change in relative proportions of each lifetime component over time for 20  $\mu\text{M}$  HO<sub>2</sub>C-Hex-Dip-Hex-C6 (black,  $\tau_1$  (shortest lived component); gray,  $\tau_2$  (mid-lifetime component); red,  $\tau_3$  (longest lived component), (C) analogous data for 20  $\mu\text{M}$  HO<sub>2</sub>C-Hex-Dip-Hex-C12.

give rise to a relatively short excimer emission lifetime. The environment giving rise to this emission is expected to be less viscous and more disordered than the more ordered/viscous states that follow 20–30 min later.

The time range of this evolution in activity is very slow relative to molecular-scale dynamics in bilayers with the exception of lipid flip-flop in which a lipid molecule migrates from one leaflet to the other within the bilayer.<sup>47</sup> With a few notable exceptions,<sup>48,49</sup> virtually every mechanistic proposal for synthetic ion channels involves transmembrane structures.<sup>1–3,5–9,20,24,26,32</sup> To achieve such structures, insertion of the transporter is required, including in many cases a process akin to lipid flip-flop in which a polar head group is required to penetrate the bilayer. Insertion of the transporter is routinely assumed to be relatively rapid but may be rate-limiting.<sup>2,5</sup> The data presented for HO<sub>2</sub>C-Hex-Dip-Hex-C6 show that activity falls off with the same time frame as lipid flip-flop, suggesting that assembly of a transport-competent aggregate does not require prior penetration of both leaflets of the bilayer and that migration though the bilayer may be detrimental to the activity of this compound.

Our alternative proposal is sketched in Figure 8, which begins as previously with injection of a compound to form a monomeric species in water (structure A) and the expected aqueous aggregate (structure B). We know experimentally that transfer from water to vesicles is rapid and that the structure produced is partially, but not fully, isolated from aqueous quenchers. An orientation which meets these criteria, and is kinetically accessible, is a U insertion in which the strand doubles on itself via a gauche conformation (structure C). The

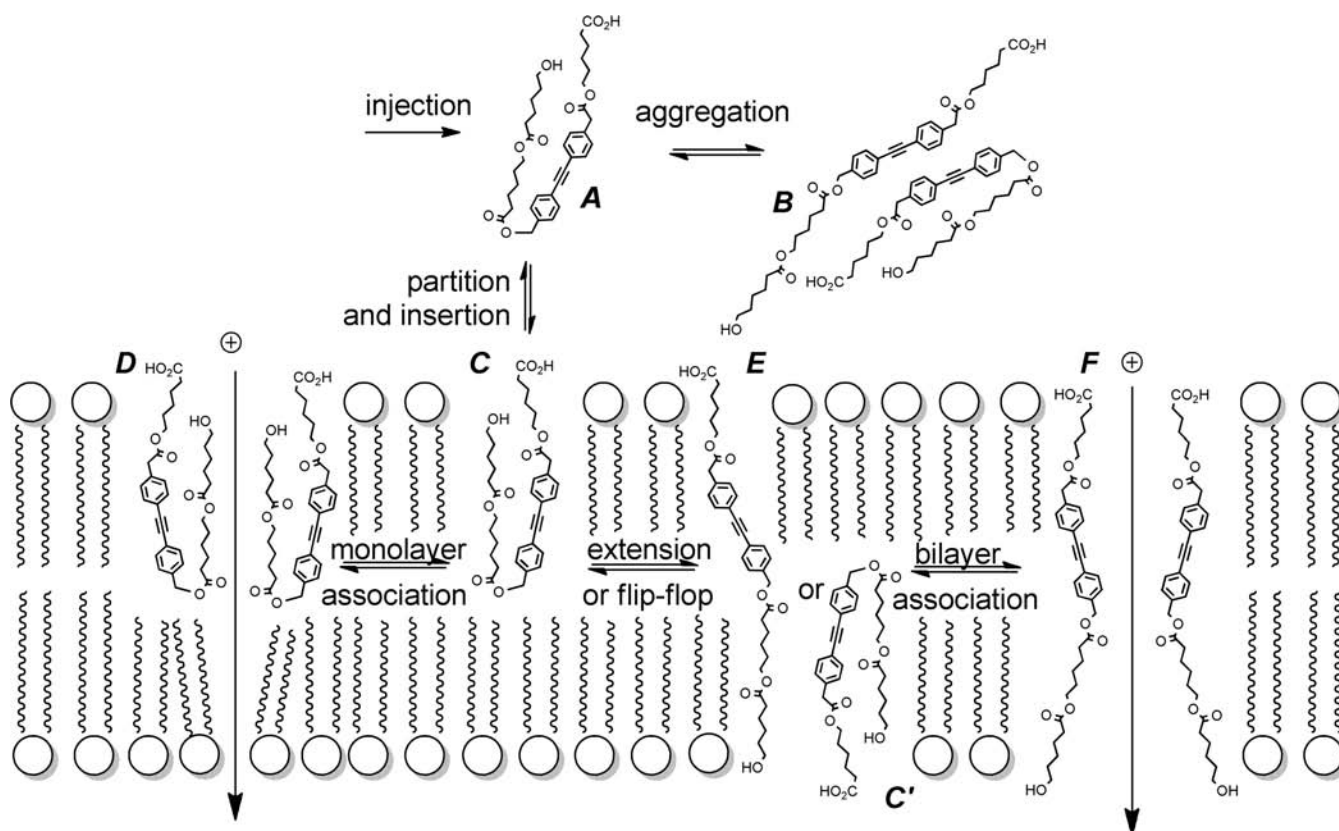


**Figure 8.** Mechanistic possibilities for the action of Dip oligoester channels.

hinge is illustrated as occurring at the hydroxyl end of the Dip unit as this point is compatible with the leaflet thickness. Alternative orientations involving a surface-associated state with the long axis of the molecule roughly perpendicular to the bilayer normal, or partially inserted L-shaped structures, cannot be excluded a priori, but the very high partition coefficients suggest a very strong hydrophobic driving force which we view as more consistent with the inserted U-shaped state. Progress from this inserted U state to a membrane-spanning state (structure E via “extension”) or U shape in the opposite leaflet (structure C’ via flip-flop) must be a slower process initially, but could be accelerated in the presence of defects or channels derived by some alternative process. That alternative we see as an association of U-shaped insertion products to form an aggregate in the leaflet on the side of injection (structure D). Such an aggregate would be accessible to aqueous-phase quenchers and would have a relatively short excimer-emission lifetime due to the lateral mobility accessible within a single bilayer. Again, associated structures involving surface-bound or partially inserted structures cannot be excluded from consideration, but structures involving insertion through both bilayer leaflets appear to be excluded by the kinetics observed.

Would a structure such as D be able to act as a channel? We think so. Activity would depend upon the perturbations such an aggregate would induce on the lipids in the opposite leaflet. A length mismatch of only a few angstroms would be sufficient to require distortions in the lipid tails on the opposite face. More importantly, we note that transport of charged species occurs under substantial electrostatic gradients. The proposed aggregate has substantially altered one face of the bilayer capacitor, presenting a focal point for local dielectric breakdown.<sup>50</sup> Local disorder opposite such an aggregate appears to

us to be inevitable. Transport mediated by disordered structures near the phase-transition temperatures of pure lipids—via so-called lipid channels—is known<sup>50</sup> and shares some characteristics of transport by synthetic channels.<sup>9,35</sup> More directly relevant are the studies of synthetic anion transporters (SAT) that are clearly inserted into one monolayer in surface studies, yet are also clearly competent to open ion-transporting channels.<sup>48,49</sup> The rate-limiting process in this system is the dissociation of an aqueous aggregate, so the subsequent steps are obscured. In the case illustrated in Figure 8, the rate-limiting processes are membrane-associated and the slow deactivation kinetics observed for HO<sub>2</sub>C-Hex-Dip-Hex-C6 implicate active structures involving only one of the bilayer leaflets.

The transport of a charged species through such a structure would involve entrance into the throat of the aggregate where partial replacement of water with interactions with the esters could occur, followed by a short passage through a defect structure in the lipid barrier on the opposite side of the bilayer driven by the gradient imposed. This section of such a channel is expected to be of small average diameter and thus of relatively low conductance, and transport would favor more readily dehydrated ions over more highly solvated ions. It would be expected to have a reasonable duration related to the stability of the perturbing aggregate in turn governed by lateral diffusion and the dissolution of the monomer into the bulk lipid of the leaflet.

This picture is still incomplete. The compounds of this study, when directly mixed in lipid, actively form channels over periods of hours. Transmembrane “barrel-stave” structures such as F in Figure 8 must also form, even with the anomalous compound HO<sub>2</sub>C-Hex-Dip-Hex-C6. The unique feature of

HO<sub>2</sub>C-Hex-Dip-Hex-C6 is solely that it cannot access such structures in vesicles. Rather it forms an inactive aggregate of some type, possibly an aggregate of C' on the inner leaflet of the vesicle bilayer, or alternatively a deeply embedded parallel aggregate similar to F.

The structures given in Figure 8 imply the orientation of the transporter but do a poor job of illustrating the nature of the channels formed. The typical conductance of the dominant type of channels formed with these compounds is on the order of 100–300 pS (Figure 4), corresponding to an apparent diameter of 3–5 Å by the Hille equation.<sup>9</sup> Such a structure requires several molecules to surround the opening, and although the added transporter is expected to provide the stabilization for the ion in transit, lipids are expected to be present as components of the channel walls, and the channel itself is expected to involve a significant amount of water. That such structures are active for periods of seconds or longer is truly remarkable considering that they are likely not maintained by specific intermolecular interactions along the walls of the channel. That the conductance of such a structure varies widely in this open period (erratic or “purple” behavior) is therefore unsurprising as the components of the structure are continually buffeted by the thermal motions of the molecules in the bilayer.

## CONCLUSIONS

The simple variations in structure within the set of compounds reported have produced a useful range of transport activities, and the incorporated Dip unit has provided a useful set of fluorescence data (steady-state and time-resolved) with which to probe the mechanisms of action. The loss of activity over a period of 20–30 min observed in one case correlated with changes in the fluorescent lifetime led us to the proposal that an aggregate within a single leaflet of the bilayer could give rise to membrane permeability. A channel of this type would involve passage of ions through defect structures in the lipid and would therefore be expected to have a relatively small diameter (low conductance) but a reasonable duration related to the lifetime of the aggregate in the opposite leaflet.

This list of expectations matches the characteristic clustering observed for a wide diversity of synthetic channels:<sup>9</sup> a dominant square-top activity of 10–30 pS conductance of ~1 s duration. We are not asserting that all reported channels involve only single-leaflet structures such as C; we are pointing out that in our system we appear to require such structures and that their characteristics by the voltage-clamp technique are of a type that is typical of many other synthetic ion channels. If insertion into a bilayer occurs by a mechanism involving one leaflet at a time and is therefore governed by the slow kinetics of flip-flop, it is reasonable to expect that transport activity associated with a single-leaflet intermediate state could appear in the voltage-clamp experimental record of virtually any potential synthetic ion channel. This commonality would give rise to the central paradox noted at the outset—that structurally diverse transporters give similar experimental results. Mechanistic proposals and structures claimed for specific synthetic channels must therefore be based on the *dissimilarity* of their behaviors with respect to “typical synthetic ion channel” behavior.

## ASSOCIATED CONTENT

### Supporting Information

Synthesis procedures and characterization of new compounds and summary conductance records of active compounds (HO<sub>2</sub>C-Hex-Dip-Hex-C6, HO<sub>2</sub>C-Hex-Dip-Hex-Hex-OH,

HO<sub>2</sub>C-Hex-Dip-Hex-Hex-OPhos). This material is available free of charge via the Internet at <http://pubs.acs.org>.

## AUTHOR INFORMATION

### Corresponding Author

tmf@uvic.ca

### Notes

The authors declare no competing financial interest.

## ACKNOWLEDGMENTS

The ongoing support of the Natural Sciences and Engineering Research Council of Canada, the University of Victoria, and The Nora and Mark DeGoutiere Memorial Scholarship is gratefully acknowledged. Funding for this research was provided by the Natural Sciences and Engineering Research Council of Canada

## REFERENCES

- (1) Davis, A. P.; Sheppard, D. N.; Smith, B. D. *Chem. Soc. Rev.* **2007**, *36*, 348–357.
- (2) Fyles, T. M. *Chem. Soc. Rev.* **2007**, *36*, 335–347.
- (3) Gokel, G. W.; Daschbach, M. M. *Coord. Chem. Rev.* **2008**, *252*, 886–902.
- (4) Gokel, G. W.; Barkley, N. *New J. Chem.* **2009**, *33*, 947–963.
- (5) Davis, J. T.; Okunola, O.; Quesada, R. *Chem. Soc. Rev.* **2010**, *20*, 3843–3862.
- (6) Mutihac, L. *Anal. Lett.* **2010**, *43*, 1355–1366.
- (7) Sansone, F.; Baldini, L.; Casnati, A.; Ungaro, R. *New J. Chem.* **2010**, *34*, 2715–2728.
- (8) Matile, S.; Vargas, A.; Montenegro, J.; Fin, A. *Chem. Soc. Rev.* **2011**, *40*, 2453–2474.
- (9) Chui, J. K. W.; Fyles, T. M. *Chem. Soc. Rev.* **2012**, *41*, 148–175.
- (10) Leevy, W. M.; Huettner, J. E.; Pajewski, R.; Schlesinger, P. H.; Gokel, G. W. *J. Am. Chem. Soc.* **2004**, *126*, 15747–15753.
- (11) Leevy, W. M.; Weber, M. E.; Gokel, M. R.; Hughes-Strange, G. R.; Daranciang, D. D.; Ferdani, R.; Gokel, G. W. *Org. Biomol. Chem.* **2005**, *3*, 1647–1652.
- (12) Leevy, W. M.; Weber, M. E.; Schlesinger, P. H.; Gokel, G. W. *Chem. Commun.* **2005**, 89–91.
- (13) Li, X.; Shen, B.; Yao, X.-Q.; Yang, D. *J. Am. Chem. Soc.* **2007**, *129*, 7264–7265.
- (14) Li, X.; Shen, B.; Yao, X.-Q.; Yang, D. *J. Am. Chem. Soc.* **2009**, *131*, 13676–13680.
- (15) Mora, F.; Tran, D.-H.; Oudry, N.; Hopfgartner, G.; Jeannerat, D.; Sakai, N.; Matile, S. *Chem.—Eur. J.* **2008**, *14*, 1947–1953.
- (16) Litvinchuk, S.; Sorde, N.; Matile, S. *J. Am. Chem. Soc.* **2005**, *127*, 9316–9317.
- (17) Andersen, O. S.; Koeppe, R. E.; Roux, B. Gramicidin Channels: Versatile Tools. In *Biological Membrane Ion Channels*; Chung, S.-H., Andersen, O. S., Krishnamurthy, V., Eds.; Springer: New York, 2007; p 658.
- (18) Pfeifer, J. R.; Reiss, P.; Koert, U. *Angew. Chem., Int. Ed.* **2006**, *45*, 501–504.
- (19) Wagner, H.; Harms, K.; Koert, U.; Meder, S.; Boheim, G. *Angew. Chem., Int. Ed. Engl.* **1996**, *35*, 2643–2646.
- (20) Sisson, A. L.; Shah, M. R.; Bhosale, S.; Matile, S. *Chem. Soc. Rev.* **2006**, *35*, 1269–1286.
- (21) Sakai, N.; Mareda, J.; Matile, S. *Acc. Chem. Res.* **2005**, *38*, 79–87.
- (22) Ma, L.; Harrell, W. A.; Davis, J. T. *Org. Lett.* **2009**, *11*, 1599–1602.
- (23) Ma, L.; Melegari, M.; Colombini, M.; Davis, J. T. *J. Am. Chem. Soc.* **2008**, *130*, 2938–2939.
- (24) Gokel, G. W.; Ferdani, R.; Liu, J.; Pajewski, R.; Shabany, H.; Uetrecht, P. *Chem.—Eur. J.* **2001**, *7*, 33–39.
- (25) Murray, C. L.; Shabany, H.; Gokel, G. W. *Phys. Chem. Chem. Phys.* **2000**, *2* (23), 2371–2372.
- (26) Gokel, G. W. *Chem. Commun.* **2000**, 1–9.



- (27) Abel, E.; Maguire, G. E. M.; Murillo, O.; Suzuki, I.; De Wall, S. L.; Gokel, G. W. *J. Am. Chem. Soc.* **1999**, *121*, 9043–9052.
- (28) Ferdani, R.; Pajewski, R.; Pajewska, J.; Schlesinger, P. H.; Gokel, G. W. *New J. Chem.* **2005**, *29*, 673–680.
- (29) Djedovic, N.; Ferdani, R.; Harder, E.; Pajewska, J.; Pajewski, R.; Weber, M. E.; Schlesinger, P. H.; Gokel, G. W. *New J. Chem.* **2005**, *29*, 291–305.
- (30) Schlesinger, P. H.; Ferdani, R.; Pajewski, R.; Pajewska, J.; Gokel, G. W. *Chem. Commun.* **2002**, 840–841.
- (31) Schlesinger, P. H.; Ferdani, R.; Liu, J.; Pajewska, J.; Pajewski, R.; Saito, M.; Shabany, H.; Gokel, G. W. *J. Am. Chem. Soc.* **2002**, *124*, 1848–1849.
- (32) Matile, S.; Sakai, N. The Characterization of Synthetic Ion Channels and Pores. In *Analytical Methods in Supramolecular Chemistry*; Schalley, C. A., Ed.; Wiley-VCH: Weinheim, Germany, 2007; pp 381–418.
- (33) Genge, K.; Moszynski, J. M.; Thompson, M.; Fyles, T. M. *Supramol. Chem.* **2012**, *24*, 29–39.
- (34) Moszynski, J. M.; Fyles, T. M. *Org. Biomol. Chem.* **2011**, *9*, 7468–7475.
- (35) Moszynski, J. M.; Fyles, T. M. *Org. Biomol. Chem.* **2010**, *8*, 5139–5149.
- (36) Luong, H.; Fyles, T. M. *Org. Biomol. Chem.* **2009**, *7*, 733–738.
- (37) Luong, H.; Fyles, T. M. *Org. Biomol. Chem.* **2009**, *7*, 725–732.
- (38) Moszynski, J. M. *The Synthesis and Characterization of Diphenylacetylene Containing Ion Channels*; University of Victoria: Victoria, Canada, 2011.
- (39) Fyles, T. M.; Hu, C.; Luong, H. *J. Org. Chem.* **2006**, *71*, 8545–8551.
- (40) Lei, X.; Porco, J. A. *Org. Lett.* **2004**, *6*, 795–798.
- (41) Gomez, C.; Chen, J.; Wang, S. *Tetrahedron Lett.* **2009**, *50*, 6691–6692.
- (42) Nishizawa, M.; Yamamoto, K.; Seo, H.; Imagawa, H.; Sugihara, T. *Org. Lett.* **2002**, *4*, 1947–1949.
- (43) Chui, J. K. W.; Fyles, T. M.; Luong, H. *Beilstein J. Org. Chem.* **2011**, *7*, 1562–1569.
- (44) Huang, Z.; Haugland, R. P. *Biochem. Biophys. Res. Commun.* **1991**, *181*, 166–171.
- (45) Hirata, Y. *Bull. Chem. Soc. Jpn.* **1999**, *72*, 1647–1664.
- (46) Lakowicz, J. R. *Principles of Fluorescence Spectroscopy*, 3rd ed.; Springer: New York, 2006.
- (47) Yeagle, R. L. *The Structure of Biological Membranes*, 2nd ed.; CRC Press: Boca Raton, FL, 2005.
- (48) You, L.; Ferdani, R.; Li, R.; Kramer, J. P.; Winter, R. E. K.; Gokel, G. W. *Chem.—Eur. J.* **2008**, *14*, 382–396.
- (49) Elliott, E. K.; Daschbach, M. M.; Gokel, G. W. *Chem.—Eur. J.* **2008**, *14*, 5871–5879.
- (50) Heimberg, T. *Biophys. Chem.* **2010**, *150*, 2–22.